

Synthesis and Characterization of Algeria Organo clays used for Elimination of Phosphate Anions from Aqueous Solution

S. Bandou^{1*}, M. Amrani¹, O. Bouras²

1. Laboratory of Soft Technology, Recovering, and Sustainable Development Faculty of Science, M'Hamed Bougara University, 35000 Boumerdes, Algeria.
2. Institute of Industrial Chemistry, University of Saad Dahleb, BP 270, 09000 Blida, Algeria.

*Corresponding author: s.bandou@univ-Boumerdes.dz; bandousamira@gmail.com

ARTICLE INFO

Article History :

Received : 20/05/2019

Accepted : 14/11/2019

Key Words:

Pillared clay; Cationic Surfactants; Characterization; Adsorption, phosphate, Kinetic.

ABSTRACT/RESUME

Abstract: This study is based on synthesis and characterization of three different clays (Sodic-bentonite noted Na – Bt , Dialyl Dimethyl Ammonium Chloride-bentonite noted DDMA – Bt and bentonite intercalated by Hexadecyl Trimethyl Ammonium Bromide or HDTMA – Bt .These three clay complexes were characterized by both Xray diffraction (XRD) and Fluorescence (XRF) Scanning Electron Microscopy (SEM), Fourier transform infrared spectroscopy (FTIR),textural measurements (BET specific surface areas and porosities) and the cationic exchange capacity (CEC).

Corresponding obtained results confirm the good intercalation of the Na – Bt by the two used surfactants at low concentrations (0.006M for HDTMAB and 0.007Mfor DDMA⁺).

Obtained results give basal spacing values around 14.5 and 18.5Å , respectively for verified two aims firstly: The originality of this research, secondly for minimized the production cost of the adsorbents.

Adsorption kinetic study of phosphate ions (PO_4^{3-}) on these three matrices was carried out using kinetic models of pseudo-first, pseudo-second-order and intraparticle diffusion. Results obtained at the studied conditions (room temperature $T = 25^\circ C$), (acidic medium $pH = 5.7$) show clearly the good validity of the pseudo-second-order model which gives a better correlation coefficient both, for DDMA – Bt ($R^2 = 0.995$) and HDTMA – Bt ($R^2 = 0.999$) compared to that obtained by Na – Bt ($R^2 = 0.990$)The aim of this present study was to evaluate the feasibility of using chicken eggshells as low-cost biosorbentfor nickel(II) ions adsorption from aqueous solutions. In order to clarify the adsorption process, batch experiments were performed to study the effect of operating parameters such as biosorbent dose (1-10 g/L), initial concentration of nickel ions (10-50 mg/L), contact time (5-120 min) and temperature (20-50 °C). To describe the adsorption equilibrium, the experimental data were analyzed by the Langmuir, Freundlich and Temkin isotherm models. The Freundlich model showed better representation of data ($R^2 > 0.999$).The maximum adsorption capacity Adsorption isotherms give adsorbed amounts of about 33 and 63 $mg.g^{-1}$ onto DDMA – Bt HDDMA – Bt complexes, respectively, and 14 $mg.g^{-1}$ for Na – Bt as reference adsorbent. These results indicated the adsorption of phosphate anions (PO_4^{3-}) by the two

prepared Algerian modified organo clays through interactions by the chemisorptions on the surface sites of each used modified clay complexes.

I. Introduction

Heavy metal pollution is an environmental problem of worldwide concern. The heavy metals are among the most common pollutants found in industrial effluents [1]. Chrome is one of toxic heavy metals and it can be present in wastewater from electroplating, refining and welding industries [2]. The chronic toxicity of chrome to humans and the environment has been well documented and high concentration of chrome causes cancer of lungs, nose and bone [3]. Several processes have been employed for the removal of chrome ions from water and wastewater including chemical precipitation, ion-exchange, membrane filtration, electrochemical treatment and adsorption [4]. environment (< 0.1% of the mass of the terrestrial rocks).

It is found it in the form of aluminum and iron, calcium phosphates in the volcanic rocks and sedimentary. On continental surfaces, the phosphates are put in solution by the deterioration of these rocks under the effect of rain water. Plants absorb solubilized phosphates and use them to produce organic matter during the process of bio synthesis. Phosphorus is then transferred along the food chain by consumption from the plants by the animals. It is again solubilized thanks to the decomposition of the matter died by the micro-organisms.

To small scale (lake, river, forest, grazing ground), phosphorus thus follows a succession of organic phases (a live world) and mineral (after decomposition of a live). On a large scale, the phosphorus introduced into the ecosystems by hydrous erosion and scrubbing are conveyed by the rivers to the coastal areas where it fertilizes littoral water. This water is generally very productive in phytoplankton marine phosphorus is found in dissolved or particulate form.

Dissolved phosphorus understands the mineral shapes of ions orthophosphates (ions mono-orthophosphates HPO_4^{2-} and di-orthophosphates H_2PO_4^- , and the organic forms in the course of mineralization of the dead matter (phosphoprotéines, phospholipids).The ions orthophosphates (classically indicated PO_4^{3-}) play a crucial role for the operation of the ecosystems because they constitute the only bio disponible

form for the plants. They are present in pore waters of the grounds and the sediments and in the water column of the aquatic environment. Taken by the plants to produce organic matter (biosynthesis), they are then released by mineralization of the matter died under the action of the heterotrophic bacterium [1].The environmental nuisances caused by phosphorus, in particular in the aquatic environments, have reinforced the interest carried to this element for several decades. One regards it as the person in charge of the process of eutrophication. Etymologically the word eutrophication means « Well nourished ».To control or mitigate eutrophication, several methods have been used to eliminate and / or reduce the phosphorus concentration below the recommended standards, thus, many methods of phosphorus have been proposed including those based on the chemical process by precipitation reaction with anions phosphorous, oxide, chlorine or metallic like iron (Fe), aluminum (Al), calcium (Ca) [2,4]. Although the chemical method remains the most reliable and easy to use, its use remains expensive because of the secondary pollution caused by the abundant production of sludge, then the biological process enhanced phosphorous removal (EDPR) [5,7]. While this process in most cases it is not sufficient to reduce phosphorous content in the effluent below 1 mgL^{-1} of total phosphorus [8].

Also several researchers have shown that the biological process has a lower overall operating cost, when compared with chemical precipitation [2,3].

The adsorption method, which has some advantages over the two previous methods, is the most preferred method for phosphorus removal. In fact, the adsorption tests on activated aluminum oxides of aluminum (Hy – Al) and iron (Hy – Fe) have made it possible to eliminate phosphate anions, by replacing natural inorganic cations with surfactant cations, the initially hydrophilic clays become hydrophobic and organophilic [9,12].Organic clay complexes or organic clays have been widely used in the adsorption of chemical pollutants, such as phosphate [13,14].

The first objective of this study is therefore the preparation and characterization of new organo-clay complexes based on an natural Algerian bentonite homoionized by sodium cations and then intercalated by two cationic surfactants at low

concentrations (0.006M HDTMA and 0.007M DDMA).

The originality of this research is to minimize production costs by using very low concentrations of surfactants in obtaining two new hydrophobic and organophilic matrices (HDTMA – Bt and DDMA – Bt). Indeed, the various previous works performed on the modification of the clays used large amounts of surfactants which therefore increase the production costs of these adsorbents.

The second part was devoted to the use of these two new hydrophobic and organophilic matrices (HDTMA – Bt and DDMA – Bt) in adsorption tests of phosphate anions (PO_4^-) in aqueous solution likely to pollute the surface waters.

II. Materials and Methods

Preparation of Na-Bentonite: The raw bentonite used in this research was purchased from National Company for Geological and Mining (province Hammam Bougrara in western Algeria). Its chemical constituents are illustrated in Table 1. The bentonite is made homoionic sodium by mixing 50g of crude bentonite in 1L of distilled water for 24 hours. After homogenization and solid/liquid separation by filtration, the solid phase was saturated with sodium ions by three treatment operations in 1M NaCl sodium chloride solution for 24 hours, and then the solid phase in the form of homoionic sodium bentonite (Na – Bt) was subjected to several successive washes with distilled water to remove the excess of the chloride ions. This washing operation is continued until the total disappearance of the chloride ions in the supernatant. The corresponding test is carried out with silver nitrate $AgNO_3$ after drying at $105^\circ C$ for two hours; the resulting Na-Bt matrix is stored in sealed plastic bottles before further use.

II.1. Cationic Surfactants: The physicochemical characteristics of the two used surfactants were presented in table 2:

Table 1. Physicochemical characteristics of the two used surfactants

Samples	DDMAC	HDTMAB
Chemical formula	$C_8H_{16}NCl$	$C_{19}H_{42}NBr$
Mark	Merk	Aldrich
Density($g.L^{-1}$)	1.04	---
Purity (%)	98	97

II.2. Pillaring reaction and preparation of intercalated bentonite clays: The pillaring process is a chemical reaction verified by the intercalation of the homoionic sodium bentonite (Na – Bt) by cation exchange process [15]. The corresponding operation consists to replace the interlamellar sodium cations (Na^+) by DDMA (diallyldimethylammonium chloride) or HDTMA (hexadecyltrimethylammonium bromide).

The preparation of intercalated bentonites clays were realized as follow:

Two suspensions were prepared separately by mixing 20 g of homoionic sodium bentonite (Na – Bt) with (0.50L) of cationic surfactant DDMA (0.007M) or HDTMA (0.006M), respectively. Each slurry was subjected to continuous stirring for 24 hours at room temperature ($25^\circ C$).

After solid / liquid separation by centrifugation at 8000 rpm and several washes with distilled water to remove excess surfactants, the two solid phases obtained, called organo-bentonite complexes designated respectively by DDMA – Bt and HDTMA-Bt HDTMA – Bt are dried at $80^\circ C$ for 60 hours. These solids are stored in dark bottles away from light before their future use.

II.3. Phosphate adsorption: The phosphate stock solutions of $20 mgL^{-1}$ was prepared by dissolving 0.286g of potassium dehydrogenate orthophosphate (KH_2PO_4) powders (analytical reagent grade) in 1L of deionized water. Phosphate solutions of desired concentrations were obtained by dilutions in $0.01 molL^{-1} KCl$ solution (KCl as background electrolyte), and the desired pH solutions were adjusted by adding a few drops of dilute solutions of NaOH or HCl.

Phosphate adsorption experiments were performed using a batch technique. A series of 100 mg samples of each used sorbent clay (Na – Bt, DDMA – Bt and HDTMA – Bt) were mixed with the same volumes (50mL) of phosphate solution with varying initial concentrations in a series of conical bottles of capacity 100mL. Before analysis and determination of the phosphorus concentration. The kinetic study and equilibrium adsorption isotherms of P on selected samples (Na – Bt, DDMA – Bt and HDTMA – Bt) were studied.

III. Methods of characterization

III.1. The X-Ray Fluorescence: the chemical composition of the raw bentonite and Na – Bt samples were conducted by X – ray fluorescence (XRF) on PHILIPS PW1480 spectrometer each sample was dried at $105^\circ C$ for 2 hours then heated

at 1000°C for 2 hours. The decrease in mass was taken as the loss on ignition (LOI).

III.2. The X-Ray diffraction: the mineralogical composition of the Na – Bt, DDMA – Bt and HDTMA – Bt samples and the spectrum were obtained using a PHILIPS PW 1710 diffractometer equipped with graphic mono chromatic CuK α radiation (1.518 Å) operated at (40k, 40A, 0.5°)

III.3. Infrared-Spectroscopy-Transformed-Fourier (FT-IR): The FT – IR spectra were determined with Spectrophotometer (FTIR Nicolet 5700, USA) by this method.

Samples for FTIR measurement were prepared by mixing 6% of specimens with 120mg of KBr powder. Mixtures were pressed into a sheer slice and the corresponding samples were analyzed with 2 cm⁻¹ resolution and were recorded between the ranges 400 – 4000cm⁻¹.

III.4. Scanning Electron Microscopy (SEM)

The morphological crystalline of the three studied samples was analyzed by Scanning Electron Microscopy (SEM). Analysis was carried out at 15kV using a (JEOL JSM – 630LV).

The specific surface areas of the three matrices were measured by adsorption of nitrogen to the BET-method on a Micrometrics 2000 apparatus. All matrices were out gassed at 250°C during 5 hours at vacuum of 10⁻⁴Torr [16].

The CEC of the three samples was determined by reagent cobalt hexane amine chloride [Cl₃CO(NH₃)₆] and colorimetric method, respectively [17].

Phosphate was analyzed by the molybdate bleu method [18]. The values for initial (C₀) and final phosphate concentration (C_e) were used to calculate the uptake capacities (q_e) as the amount of phosphate sorbet at equilibrium per amount of powder sample (mg g⁻¹). All analyses were carried out in triplicate.

IV. Results and discussion

IV.1. Determination of chemical composition by fluorescence X

From the results in table1, X – ray fluorescence analysis indicated that the two samples (raw bentonite and sodium bentonite) are composed mainly of silicates (SiO₂), alumina (Al₂O₃) other such as K₂O, Fe₂O₃, TiO₂ and exchangeable cations such as calcium (Ca²⁺), Sodium (Na⁺) and Magnesium (Mg²⁺). These results are comparable to those reported earlier by [19].

Results show an increase in the sodium level from 1.74 in the crude bentonite to 3.97 in sodium homo ionic clay

(Na – Bt). After purification and sodium homoionization, the values of the (SiO₂/Al₂O₃) ratio increased respectively from 2.72 to 3.76, characterizing the montmorillonite fraction and showing a good concordance with the results reported previously [20].

Table 2. Chemical composition of the used clay Samples

Chemical Composition (%)	Raw Bentonite (Bt)	Sodic Bentonite (Na-Bt)
SiO ₂	54.19	58.10
Al ₂ O ₃	16.78	15.42
Fe ₂ O ₃	2.00	1.92
Na ₂ O	1.74	3.97
CaO	1.06	0.69
MgO	3.04	2.82
K ₂ O	1.95	1.45
P ₂ O ₅	0.04	----
TiO ₂	0.11	0.16
SO ₃	0.11	----
PAF	19.48	14.91
SiO ₂ /Al ₂ O ₃	3.23	3.76

The results of mineralogical composition are presented by XRD diagrams (2 θ values from 2 to 60°) for the three studied samples are illustrated in the Figure1, they suggest that firstly: this clay is predominantly composed of montmorillonite at the peaks (2 θ = 6.89°, 19.80°, 21°) for the Na – Bt, (2 θ = 6.22°) for DDMA – Bt, and (2 θ = 4.90°) for HDTMA – Bt, the other peaks were attributed to impurities such as albite, orthoclase, and quartz for the three used clays as shown in table3. Secondly: they show increases in the basal spacing (d₀₀₁) of 12.71Å (for Na – Bt) up to 14.55Å (for DDMA – Bt) and 18.48Å (for HDTMA – Bt), indicating intercalation by a cation exchange mechanism [15]. These values indicate that the chains of the two used cationic surfactants are intercalated elongated horizontally and parallel to the clay layer either in DDMA – Bt monolayer or bilayer for HDTMA – Bt [21]. These results thus confirm the formation of two types of hydrophobic and organophilic organo-clay complexes.

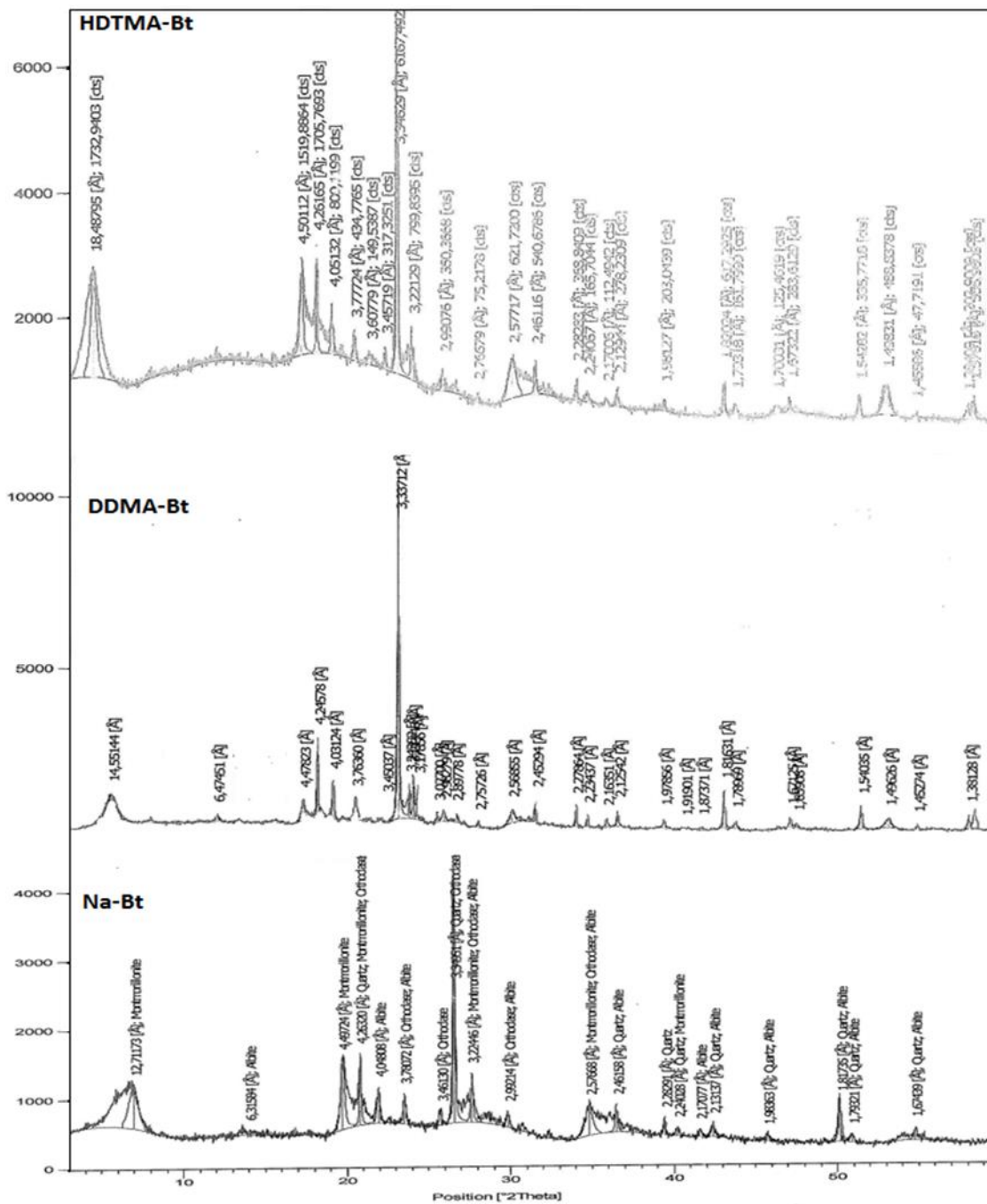


Figure 1. X-ray diffraction patterns of the studied clay samples Na-Bt (A), DDMA-Bt (B) and HDTMA-Bt (C).

Table 3. The mineralogical composition of the impurities of the three used clay Samples

Samples	$2^{\circ}\theta$	$d_{001}[A^{\circ}]$	Impurities
Na-Bt	13.5°,20°,1°,21.8°,23.8°,25.8°,26.9°,28°,30°,35°,36.5°,39.50°,40°,40.5,41.8,42,45.8,50,51, 55.90°.	6,31,4.49,4.26,4.04,3.78,3.46,3.34,3.22,2.99,2.572.46,2.28,2.24,2.17,2.13,1.81,1.79,1.67.	Albite. Orthodase and the Quartz.
DDMA-Bt	13.8,20.21,21.8,23.9,25.80,26.9,27.8,29.2,30,31,32.5,34.90,36.8,37.2,39,8,40.3,42,42.5,46,47.648,5,50,51,55.	6.47,4.47,4.24,4.03,3.76,3.45,3.33,3.17,3.02,2.89,2.56,2.45,2.27,2.23,2.16,2.12,1.97,1.91,1.87,1.81,1.78,1.60	Albite.Orthodase and the Quartz.
HDTMA-Bt	19.9,20.9,22,23.8,24.9,25.8,26.9,27.8,30,32.5,34.8,,37,39.8,40.5,41.7,42.5,46,50,50.8,51,54,55.5.	4.50,4.05,3.77,3.60,3.45,3.34,3.22,2.99,2.76,2.572.46,2.28,2.24,2.17,2.12,1.98,1.82,1.79,1.67,1.54.	Albite.Orthodase and the Quartz.

Concerning the results of the values of the cation exchange capacity (C.E.C) and those of the specific surface area for the three studied clay samples as shown in the table 4, So the decreases observed in the values of the cation exchange capacity because the coverage of permanent charge on the surface of the Na-Bentonite by alkylic chain carbonyl for the two surfactants by the mechanism of exchanged capacity cations by the replaced the sodium cations by carbonyl chain alkylic of the two surfactants where such as their atomic rays are less compared to the atomic rays of sodium cations rendered the decreases in the CEC of the organophilic clays [12] in the first hand so in the second hand the decrease of specific surface areas of each pillar clay sample is explained by the fact that the internal surfaces of the sodium bentonite are filled by two organic surfactants used and that the molecules of the N_2 gazes could not reach these internal surfaces which remain blocked

by these large interlamellar alkyl chains as previously proposed [22].

Table 4. CEC and BET analysis results of the three used clay samples

Samples	CEC (meq/100 g)	BET Specific surface area (m^2g^{-1})
Na-Bt	74	88
DDMA-Bt	51	34
HDTMA-Bt	32	18.53

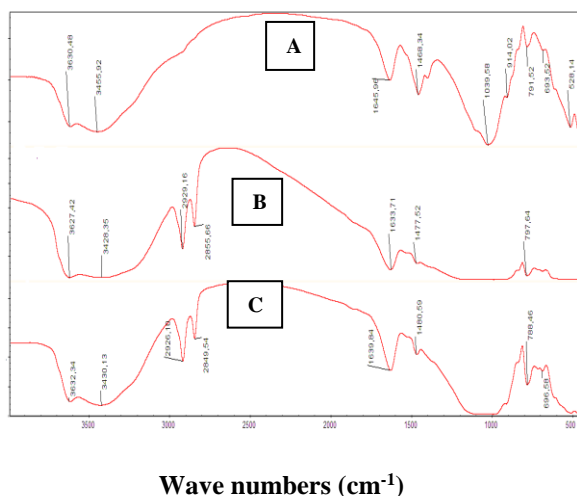
IV.2. FTIR measurements

The FTIR spectra results are presented in the Figure 2 (A), Figure 2 (B) and Figure 2 (C), of the Na – Bt, DDMA – Bt and HDTMA – Bt samples recorded between 500 and 3500 cm^{-1} show the following phenomena:

The absorption bands at 3456.92 cm^{-1} , 3428 cm^{-1} and 3430 cm^{-1} are attributed to the OH stretching vibrations for the water molecules adsorbed on the surface of the clay. The others located at 3424 cm^{-1} , 3627 cm^{-1} and 3621 cm^{-1} represent the stretching vibrations of the OH groups coordinated with the octahedral Al^{3+} cations in the Na – Bt, DDMA – Bt and HDTMA – Bt samples, respectively [23].

The bands centered at 528 cm^{-1} and 519 cm^{-1} are due to the stretching vibrations of the, Si – O – Si groups present in the used bentonites. The new bands appearing at 2929 cm^{-1} and at 2926 cm^{-1} are attributed to the $CH_3 - N$, stretching vibrations of the surfactants [20]. And those appearing at 2856 cm^{-1} and 2849 cm^{-1} concern the stretching vibrations of the symmetric CH_2 groups of intercalated clays DDMA – Bt and HDTMA – Bt.

The others new wave bands appearing at 1477 cm^{-1} and 1480 cm^{-1} correspond to ammonium ions [21]. The intercalation of the two alkyl ammonium in the interlamellar spaces by ion exchange is confirmed by the appearance of these new bands and the decrease of the intensity of the bands 1640 cm^{-1} , 1633 cm^{-1} corresponding to the modes of bending of the water.



Wave numbers (cm⁻¹)
Figure 2. Infrared Transformed Fourier Spectrum (FT-IR) of the Na-Bt (A), DDMAC-Bt (B), and HDTMAB-Bt (C).

IV.3. SEM analysis: The morphological crystalline results of the three studied samples by Scanning Electron Microscopy (SEM) are explained by: in the first as shown in the Figure 3 (A), the Na – Bt micrograph shows darker lines in the matrix which is brighter due to the presence of heavier elements, including Al, Si and O in the composition of layers of clay. Sintering lighter sodium atoms of the raw bentonite are shown through the white phases.

However, clays intercalated with organic surfactants Figure 3 (B) and Figure 3 (C) show significant changes in morphology. This gives a much smoother surface structure. In fact, the appearance of parallel superimposed light fragments in the darker lines with fragments of smaller sizes indicates the presence of lighter atoms such as O, H and N characterizing the two intercalated cationic surfactants [24].

matrix which is brighter due to the presence of heavier elements, including Al, Si and O in the composition of layers of clay. Sintering lighter sodium atoms of the raw bentonite are shown through the white phases.

However, clays intercalated with organic surfactants Figure 3 (B) and Figure 3 (C) show significant changes in morphology. This gives a much smoother surface structure. In fact, the appearance of parallel superimposed light fragments in the darker lines with fragments of smaller sizes indicates the presence of lighter atoms such as O, H and N characterizing the two intercalated cationic surfactants [24].

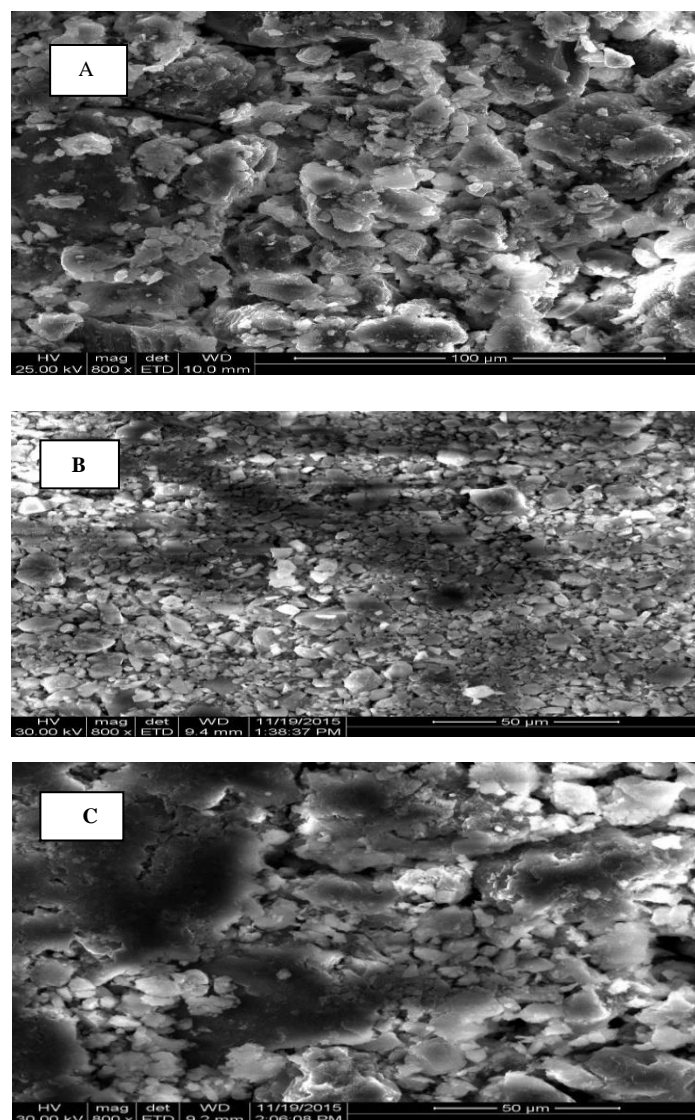


Figure 3. SEM images of Na-Bt (A), DADMA-Bt (B), and HDTMA-Bt (C)

IV.4. Adsorption kinetics of phosphate anions:

The kinetic study is very important to determine the adsorption process to predict the capability of adsorbent to remove the phosphate ions. All obtained curves have similar characters, showing an important and fast adsorption, between $t = 0$ and 50min, and a slower adsorption until equilibrium is accomplished. It can be observed (Figure4), and then the magnitudes of phosphate ions on all surfactant modified bentonite are larger than that on Na – Bt, which can be ascribed to the hydrophobic effect and electrostatic attraction [25]. Especially, the equilibrium adsorption capacity of phosphate ions on HDTMA – Bt is larger than that on DDMA – Bt, indicating that Na-Bt modified by

cationic surfactant with long alkyl chain is more favorable to the adsorption of phosphate ions. This phenomenon can be explained that the surface charge of adsorbent plays a significant role in the adsorption of ionisable matters. It has been pointed that larger HDTMA – Bt was initially treated by cation exchange in the interlayer, which caused extensive clay aggregation [26,27]. To better understand the adsorption kinetics, the adsorption data of phosphate were analyzed using kinetic models such as pseudo-first order (equation1), pseudo-second-order (equation2), and intraparticle diffusion (Equation3).

$$\frac{dq_t}{dt} = k_1(q_e - q_t) \quad (1)$$

$$\frac{dq_t}{dt} = k_2(q_e - q_t)^2 \quad (2)$$

$$q_t = k_{int}^{0.5} + C \quad (3)$$

Where:

- q_t (mg/g) is the adsorbed amount at time t ;
- q_e (mg/g) is the adsorbed amount at equilibrium;
- k_1 (mg/g(min)) is the equilibrium rate constant of the pseudo-first-order kinetics model;
- k_2 (mg/g(min)) is the equilibrium rate constant of the pseudo-second-order kinetics model;
- k_{int} (mg/g.m^{1/2}) rate constant of intraparticle diffusion;
- C (mg/g) Intercepts.

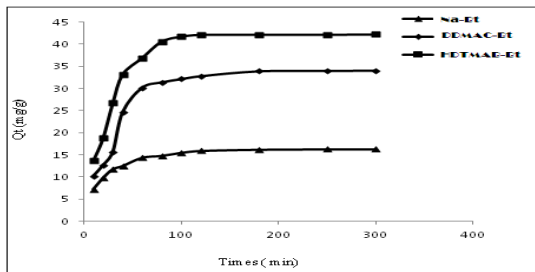


Figure 4. Kinetic study of phosphate adsorption onto Bt-Na (▲), DADMAC-Bt (◆) and DTMAB-Bt (■) according to time

Integrating equation (1) for the boundary condition $t = 0$ to $t = t$ and $q_t = 0$ to $q_t = q_t$ it was rearranged to obtain a linear form:

$$\ln(q_e - q_t) = \ln q_e - k_1 t \quad (4)$$

The values of q_e , k_1 and the correlation coefficients were determined from the linear plots of $\ln(q_e - q_t)$ versus t are presented in the Figure 5.

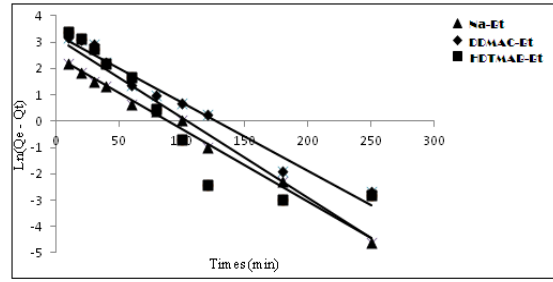


Figure 5. Kinetic modeling of phosphate adsorption on Bt-Na (▲), DADMAC-Bt (◆) and DTMAB-Bt (■) using pseudo-first-order model

Integrating equation for the boundary condition $t = 0$ to $t = t$ and $q_t = 0$ to $q_t = q_t$ it was rearranged to obtain a linear form:

$$\frac{t}{q_t} = \frac{1}{k_2 q_e^2} + \frac{t}{q_e} \quad (5)$$

The values of q_e , k_2 and the correlation coefficients were determined from the linear plots of $\frac{t}{q_t}$ versus t (Figure 6), from which the kinetic data were calculated and given in Table 5.

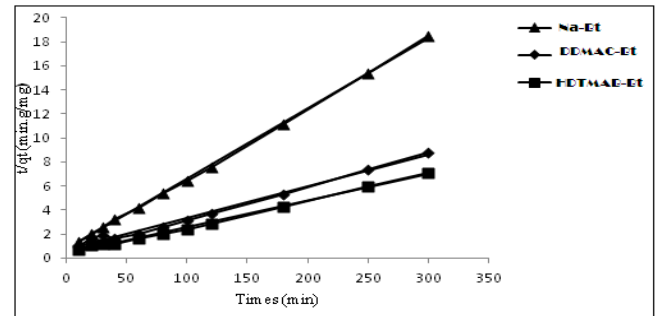


Figure 6. Kinetics modeling of phosphate adsorption on Bt-Na (▲), DDMAC-Bt (◆) and HDTMAB-Bt (■) using pseudo-second-order model.

The pseudo-first-order and pseudo-second-order kinetic models cannot by themselves identify the diffusion mechanism Kinetic data were therefore analyzed using the intraparticle diffusion model. According to this model, the plot of q_t versus the square root of time, $t^{1/2}$, for the adsorption PO_4^- onto bentonite (Figure7) from which the kinetic data were calculated and given in table 5.

Table 5.(1.2.3). Kinetic parameters for the adsorption of phosphate onto Bt-Na, DADMA-Bt, and HDTMA-Bt

Tables 5.1.

Adsorbents	q(mg.g-1)	Pseudo-first-order model		
		K ₁ (1/g.min)	q _e (mg.g ⁻¹)	R ²
Na-Bt	16.21	11.59	0.993	0.0045
DDMAC-Bt	34.04	27.58	0.972	0.001
HDTMB-Bt	42.18	23.90	0.851	0.001

Tables 5.2.

Adsorbents	q(mg.g-1)	Pseudo-second-order model		
		K ₁ (1/g.min)	q _e (mg.g ⁻¹)	R ²
Na-Bt	16.21	0.0045	17.24	0.990
DDMAC-Bt	34.04	0.001	38.46	0.995
HDTMB-Bt	42.18	0.001	45.45	0.999

Tables 5.3.

Adsorbents	q(mg.g ⁻¹)	Intraparticle diffusion model		
		K ₁ (1/g.min)	q _e (mg.g ⁻¹)	R ²
Na-Bt	16.21	0.563	8.36	0.671
DDMAC-Bt	34.04	1.684	10.63	0.711
HDTMB-Bt	42.18	1.834	17.25	0.747

The correlation coefficients for the pseudo-second-order kinetic model obtained for all studied adsorbent were found to be extremely high (> 0.990) (table5) and the calculated q_e values obtained from this equation were also close to experimental data generally. These results indicate that the adsorption process obeys the pseudo-second order kinetic model. The good agreement of the data with the pseudo-second order kinetic model suggests that the sorption process is chemical process by attraction of phosphates anions to ammonium cations of the two organoclays then the formation of imolecular bond between

phosphates anions and ammonium cations of organoclays, so could be a limiting step [28].

The q_e values for Na – Bt, DDMA – Bt and HDTMA – Bt were around 17,38 and 45 mg.g⁻¹, respectively. These values were confirmed the adsorption of phosphates anions by the sodic and organo clays then making it possible to provide the following preferential sequence: HDTMA – Bt > PDADMA – Bt > Na – Bt.

According to the intraparticle diffusion model, the plot of uptake, q_t, versus the square root of time, t^{1/2}, should be linear if the intraparticle diffusion is involved in the adsorption, and if these lines pass through the origin, and then intraparticle diffusion is the rate controlling step, otherwise this indicates that two or more steps occurred in the adsorption process.

The graphs shown in Figure 7 present two lines indicating that two steps have taken place.

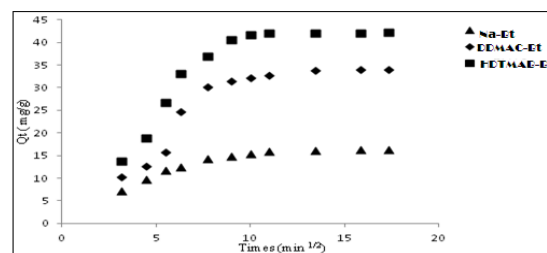


Figure 7. Intraparticle diffusion model for the adsorption of phosphate onto Bt-Na (▲), DDMAC-Bt (◆) and HDTMAB-Bt (■)

As can be seen in Figure7, the first step described progressive adsorption from 0 to 8min, where intraparticle diffusion by electrostatic force mechanism between the phosphates anions and the surface of the sodic clay then the formation of the NaHPO₄-Bentonite complex, and by electrostatic attraction mechanism between the phosphates anions and the ammonium cations of the two surfactants (DDMAC, HDTMAB), intercalated into the sodic clay, then the formation of all complexes C₈H₁₆-NPO₄-Bentonite, C₁₉H₄₂-NPO₄-Bentonite respectively confirmed the formation of into inner sphere complexes [12].

The second step is attributed to the final equilibrium step, in which the intraparticle diffusion begins to slow down due to the decrease in the concentration of the mono phosphate anions PO₄⁻ in solution. The slope of the first stage characterizes the velocity parameter which corresponds to the intraparticle diffusion, and the interception is proportional to the thickness of the boundary layer. The R₂ values of the

intraparticle diffusion model are lower than those of the pseudo-second order kinetic model, but this model indicates that the mono phosphate anions PO_4^- adsorption on bentonite can follow the intraparticle diffusion model up to 8min. This implies that intraparticle diffusion is involved in the adsorption process and is not the only step controlling the rate.

Sorption isotherms: The adsorption capacities of phosphate (q_e) on the Na – Bt, DDMA – Bt and HDTMA – Bt samples at different concentrations of phosphate in solution (C_e) are shown in Figure 8.

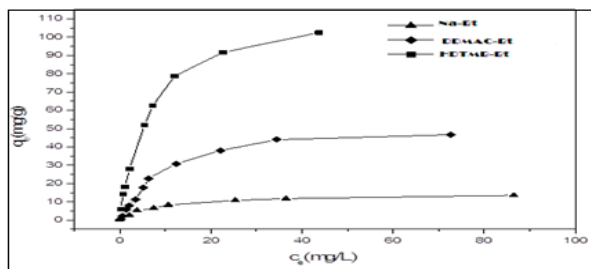


Figure 8. Effect of equilibrium concentration on Bt-Na (\blacktriangle), DDMA-Bt (\blacklozenge) and HDTMAB-Bt (\blacksquare) at $PH= 5.7$ and $T= 25^{\circ}C$

Adsorption isotherms indicate that the retention of phosphate ions increases as the concentration of phosphate ions increases. The two isotherms clearly show a rapid increase in adsorption capacity in the same direction as the equilibrium solution concentration, followed by an equilibrium plateau, demonstrating isothermal characteristics typical of Langmuir.

In order to better understand the adsorption mechanism, the Langmuir and Freundlich equations expressed in equations (6) and (7) were used to model these experimental adsorption data.

$$q_e = \frac{K_L q_m C_e}{1 + K_L C_e} \tag{6}$$

$$q_e = K_f C_e^{1/n} \tag{7}$$

Where:

C_e (mg/L) is the equilibrium adsorbate concentrations in the aqueous; q_e (mg/g) is the equilibrium adsorbate concentrations in the solid phases; q_m (mg/g) is the maximum adsorption capacity;

K_L (L/g) is the Langmuir adsorption equilibrium constant; K_f is the Freundlich equilibrium constant indicative K_L (L/g) is the Langmuir adsorption equilibrium constant; K_f is the Freundlich equilibrium constant indicative of adsorption capacity; $(1/n)$ is the Freundlich adsorption constant, the reciprocal of which is indicative of adsorption intensity.

The Langmuir isotherm equation can be rearranged to the linear form given below:

$$\frac{C_e}{q_e} = \frac{C_e}{q_m} + \frac{1}{K_L q_m} \tag{8}$$

q_m and K_L can be calculated from the slope and intercept of the linear plot with $\frac{C_e}{q_e}$ versus C_e .

Based on the Langmuir equation, a dimensionless constant called equilibrium parameter and representing the separation factor is commonly used to predict whether a sorption system is favorable or unfavorable. The Langmuir equation is applicable for homogeneous adsorption, where the sorption of each sorbate molecule onto the surface has equal sorption activation energy [29].

The Freundlich isotherm equation can be rearranged to the linear form given below:

$$\text{Log } q_e = \text{Log } K_f + \frac{1}{n} \text{Log } C_e \tag{9}$$

K_f and n can be calculated from the slope and intercept of the linear plot with $\text{Log } q_e$ versus $\text{Log } C_e$.

The values of n indicate the degree of non linear between phosphate solution concentration and adsorption [30].

$n < 1$ adsorption process is chemical; $n = 1$ linear adsorption is linear; $n > 1$ adsorption is favorable physical.

The Freundlich equation is employed to describe heterogeneous systems and reversible adsorption and is not restricted to the formation of mono layers [31]. Table 6 summarizes the constants of Langmuir and Freundlich adsorption isotherms on the three bentonite samples.

Table 6. Constants of Langmuir and Freundlich and regression coefficients for adsorption of Phosphate onto Bt-Na, DDMA-Bt, and HDTMA-Bt

Parameters	Na-Bt	DADMA-Bt	HDTMA-Bt
K_f	2,33	3,72	5,48
n	2,19	1,62	1,3
R^2	0,978	0,918	0,826
q_m (mgg ⁻¹)	13,89	33,33	62,5
K_L (Lmg ⁻¹)	0,233	0,016	0,273
R^2	0,986	0,988	0,996

The maximum adsorption capacities (q_m) calculated from the Langmuir model are respectively of the order of 14,33 and 62 mg/g for the adsorbent matrix Na – Bt, DADMA – Bt and HDTMA – Bt. This value is greater in the organo clays compared to the sodic clay because the adsorption of phosphate anions by electrostatic force mechanism from the sodic clay and by electrostatic attraction mechanism for the two organo clays.

The values of the correlation coefficient R^2 , P equilibrium sorption on the three clays (Na – Bt, DDMA – Bt and HDTMA – Bt) could be much better described using the Langmuir model than using the Freundlich one. Similar results have been reported previously in adsorption phosphate on hydroxyaluminium- and hydroxyiron-montmorillonite complexes [13].

The values of the q_m and K_f parameters calculated and compiled in table 6 allowed us to classify the efficiencies according to the following sequential order: HDTMA – Bt > DDMA – Bt > Na – Bt. In addition, the HDTMA – Bt adsorbent is characterized by a high K_L value. This is linked to the binding energy and shows that the phosphate ions adsorbed on this adsorbent are more difficult to desorb. Similar results relating to the phosphate sorption capacity were obtained from the Freundlich model (K_L value). The parameters n of the Freundlich and K_L equation of the Langmuir model are not directly comparable. Indeed, the parameter K_L of the Langmuir model measures the affinity of the adsorbent for the solute (a lower value for $K_L < 1$ indicates that the adsorption process is chemical).

On the other hand, the constant n of Freundlich is related to the interaction between the exchange sites of the adsorbent and the phosphate ions.

V. Conclusions

This work led to the Algerian clay removing of phosphate anions (PO_4^{3-}) from aqueous solutions, the characterization results by chemical by (fx) indicated that the bentonite raw bentonite and sodic bentonite are composed mainly of montmorillonite (silicates, aluminium, iron, and magnesium) and the impurities, mainly quartz, orthoclase, then the chemical analyzes for the purified sodic bentonite confirmed a good purification by increasing in the level of the sodium ions get up to 3.79 after

The purification of the raw bentonite by the exchange capacity cationic (C.E.C) also the values of the (SiO_2/Al_2O_3) ratio increased respectively from 2.72 to 3.76 characterizing the montmorillonite fraction.

The increasing in the basal spacing of the two pillared clays by DDACl and HCTMABr

(14.90°A, 18.48A°) comparing to the sodic clay, confirmed the intercalated of the two surfactants (DDACl and HCTMABr) into sodic clay by the exchanged capacity cationic justified by the mineralogical technique (DRX).

Apparition of the novel bands absorption of the two intercalated bentonite by the two surfactants $CH_3 - N$, CH_2 , NH_4 respectively informed also the insertion of the two surfactants into basal spacing of the sodic bentonite.

The changed in the morphological of the organoclays comparing to the sodic bentonite confirmed by scanning electro microscopy (SEM) analysis. The textural analysis by the BET method allowed us to confirm the creation of a dense microporous network and very low compared to the sodic bentonite.

The decreases in the capacity exchanged cationic was confirmed by colorimetric analysis.

Increasing of the adsorption of phosphate anions into organ clays by the formation of legand – exchange results the formation of into inner sphere complexes comparative to the sodic clay in the sequential order:

HDTMA – Bt > DADMA – Bt > Na – Bt.

The kinetic of phosphate anions (PO_4^{3-}) adsorption on the organo clays, could be well described using both pseudo-second order.

The adsorption capacities of the PO_4^{3-} into HDTMA – Bt clay were greater than those of the DADMA – Bt and Na – Bt which could be attributed the increasing of alkylic carbonyl chain of the HDTMA – Br comparative to DDACl.

The equilibrium adsorption of phosphate anions on the organo clays could be well described using the Langmuir isotherm.

Finally the results of characterization by (FX, DRX, IRTF, BET, CEC) confirmed the preparation of organo clays in the first, then secondly the results of the kinetic study and adsorption isotherms of phosphate anions in aqueous solution also confirmed the effectiveness of organo-bentonite complexes in the removal of phosphates in the following sequential order: HDTMA-Bt > DADMA-Bt > Bt-Na.

VI. References

1. Némery Garnier, J. The fate of phosphorus *Nature Geoscience*, 9 (2016) 343-344.
2. Levlin, E.; Hultman, B. Phosphorus recovery from phosphate rich Side streams in wastewater treatments. Proceedings of a Polish-Swedish seminar, Report:No10., Joint Polish-Swedish Reports, Gdansk Poland (2003).
3. Gullet, B.; Mc Lelland, J.; Padgett, D. System-wide planning for phosphorus reduction at Charlotte's three largest waste water treatment plants. Proceedings of South Carolina. Environmental Conference, Columbia, 2003.

4. Yousef, L.; Achour, S. Elimination of the phosphate by physico-chemical processes. *LARHYSS Journal*, ISSN: 1112-3680,4(2005)129-140.
5. Lee, S. E.; Kim, K.S.; Ahn, J.H.; Kim, C.W. Comparison of phosphorus removal Characteristics between various biological nutrient removal processes. *At SciTech*. 36 (12) (1997) 61-68.
6. Smolders, G.J.F.; Van Loos drecht, M.C.M.; Heijnen, J.J. Steady-state Analysis to evaluate the phosphate removal capacity and acetate requirement of biological phosphorus removing main stream and side stream process configurations. *Wat. Res* 30 (11) (1996)2748-2760.
7. Wild, D.; Kisliakova, A.; Siegrist, H. P-fixation by Mg, Ca and zeolite during stabilization of excess sludge from enhanced biological P-removal. *Wat. Sci. Tech*. 31 (1-2) (1996) 391-398.
8. Matsch, L.C.; Drnevich, R.F. Biological nutrient removal in *Advances in Water and Waste Treatment, Ann. Arbor. Sci.* (1987).
9. Donnert, D.; Salecker, M.; Donnert, D.; Salecker, M. Elimination of phosphorus from municipal and industrial waste water. *Wat. Sci. Tech*. 40 (4-5) (1999) 195-202.
10. Brattebø, H.; Edward, H. Phosphorus removal by granular activated aluminum. *Wat. Res*. 20 (8) (1986) 977-986.
11. Hano, T.; Takamashi, H.; Hirata, M.; Urano, K.; Shunji. Removal of phosphorus from waste water by activated alumina adsorbent. *Wat. Sci. Tech*. 35 (7) (1997)39-46.
12. Mao-Xu, Zhu.; Kui-Ying, Ding.; Shao-Hui, Xu.; Xin, Jiang. Adsorption of phosphate on hydroxyaluminum and hydroxyiron –montmorillonite complexes, *Journal of Hazardous Materials* 165 (2009) 645-651.
13. Zamparas, Miltiadis.; Areti, Gianni.; Stathi, Panagiota.; Deligiannakis, Yiannis.; Zacharias, Ierotheos. Removal of phosphate from natural waters using innovative modified bentonites. *J. Applied Clay Science*. (2012)101-106.
14. Tanyol, Mehtap.; Yonten, Vahap.; Demir, Veyse. Removal of phosphate from aqueous solutions by chemical –and thermal-modified bentonite clay. *J. Water, Air & Soil Pollution, Springer Link*. (2015) 1-10.
15. Ahmad, M.B.; Hoidy, W. H.; Ibrahim, N.A.B.; Al-Mulla, E.A.J. Modification of montmorillonite by new surfactants. *J. Eng. Appl. Sci*. 4 (3)(2009) 184-188.
16. Bouberka, Z.; Kacha, S.; Kameche, M.; Elmaleh, S.; Derriche, Z. Sorption study of aqueous solutions using modified clays. *Journal of Hazardous Materials*. B.119 (2005)117-124.
17. Bardon, C. Recommendations for the experimental determination of the capacity of exchange of the cations of the argillaceous mediums. (1983) Review IFP 38.
18. Lin, Y. The Criteria Analysis Methods of Wastewater [M]. Beijing. *The Environmental Science Publishing House of China* (2002) 332-334.
19. Makhokhi. Modification of the raw bentonite by several organic salts–applications for oils decoloration and adsorption of textiles dyes. (2008), phd disso, university of Telemcen.
20. Bouras, O. Adsorbent decorated clay properties organophiles. Synthesis and Characterization. (2003), phd disso, university of Blida.
21. Su, J.; Huai-Guo, Huang.; Xiao-Ying, Jin.; Xiao, Lu.; Zu-Liang, Chen. Synthesis characterization and kinetic of surfactant-modified bentonite used to remove As(III) and As(V) from aqueous solution, *Journal of Hazardous Materials*. 185 (2011) 63-70.
22. Zaghouane. Boudiaf, Hassina. Préparation et caractérisation de matériaux à base d'argile algérienne. Application à l'adsorption de polluants organiques, Thèse de doctorat en Génie Chimique. Université de Ferhat Abbas Sétif. (2011).
23. Önal, M., and Sarikaya, Y. Preparation and Characterization of Acid-Activated Bentonite Powders, *Powder Technology*. 172 (2007)14-18.
24. Olad, A.; Rashidzadeh, A. Preparation and anticorrosive properties of PANI/Na-MMT and PANI/O-MMT nanocomposites. *Prog. Org. Coat.* 62 (2008) 293-298.
25. Ho, Y.S. and G.McKay, Pseudo-Second Order Model for Sorption Processes, *Process Biochemistry* 34 (1999) 451-465.
26. Gammoudi, S.; Frini-Srasra, N.; Srasra, E. Influence of exchangeable cation of smectite on HDTMA adsorption Equilibrium, kinetic and thermodynamic studies. *Applied Clay Science* (2012) 69-99.
27. Zatta, Leandro.; Ramos Luiz, Pereira.; Wypych, Fernando. Acid-activated montmorillonite as heterogeneous catalysts for the esterification of lauric acid with methanol. *Applied Clay Science* 80 (2013)236.
28. Daimei, Chen.; Jian, Chen.; Xinlong, Luan.; Haipeng, Ji.; Xia, Zhiguo. Characterization of anion-cationic surfactants modified montmorillonite and its application for the removal of methyl orange. *Chemical Engineering Journal*. 171 (2011) 1150-1158.
29. Lopeza, D. G.; Gobernado-Mitre, I.; Fernandez, J. F.; Merino, J. C.; Pastor, J. M.; *Polymer*. 46(2005) 2758-2765.
30. Kundu, S. and Gupta, A.K. Arsenic Adsorption onto Iron Oxide-Coated Cement (IOCC): Regression Analysis of Equilibrium Data with Several Isotherm Models and Their Optimization. *Chemical Engineering Journal*, 122 (2006)93-106.
31. Yusof, A. M.; Keat, L. K.; Ibrahim, Z. Kinetic and Equilibrium Studies of the removal of ammonium ions from aqueous solution by rice husk ash –Synthesized zeolite Y and powdered and granulated forms of modernite. *Journal of Hazardous Materials*, 174 (1-3) (2010) 380-385.

Acknowledgment

Acknowledgements to the Ministry of Research, Scientific and Higher Education of the Republic of Algeria, and also for Chemical Engineering Department, Especially Laboratory of Soft Technology, Recovering, and Sustainable Development Faculty of Science, M'Hamed Bougara University, 35000 Bumerdes, Algeria.

Please cite this Article as:

Bandou S., Amrani M., Bouras O., Synthesis and Characterization of Algeria Organo clays used for Elimination of Phosphate Anions from Aqueous Solution, *Algerian J. Env. Sc. Technology*, 6:1 (2020) 1224-1235